THERMOSTRUCTURAL APPLICATIONS OF HEAT PIPES FOR COOLING LEADING EDGES OF HIGH-SPEED AEROSPACE VEHICLES

Charles J. Camarda
NASA Langley Research Center
Hampton, VA

David E. Glass
Analytical Services and Materials
Hampton, VA

INTRODUCTION

Stagnation regions, such as wing and engine leading edges and nose caps, are critical design areas of hypersonic aerospace vehicles because of the hostile thermal environment they experience during flight. The high local heating and aerodynamic forces cause very high temperatures, severe thermal gradients, and high stresses. In addition, as a hypersonic vehicle travels through the earth's atmosphere, the stagnation regions are subjected to a potentially severe oxidation and erosion environment. A further concern is that thermal-structural distortions may be large enough to interact with the fluid flow and cause coupling between the fluid, thermal and structural responses.

Design considerations for hypersonic aerospace vehicles can become extremely complex as the disciplines involved in the analysis and design of the vehicle become coupled. An air-breathing, single-stage-to-orbit vehicle, such as the National Aero-Space Plane (NASP), is subjected to severe aerothermal and acoustic loading; and yet many diverse, and often conflicting, design requirements must be satisfied. Mass is of critical importance to any hypersonic vehicle, in particular if the vehicle travels to orbit. The selection of the structural concepts, materials, and, if necessary, method of cooling (passive, ablative, active, and "semi-active" or heat-pipe cooling) strongly influence vehicle mass. The structural concepts and materials selected must satisfy structural, thermal, material and manufacturing requirements. Additional performance requirements such as reusability, reliability, and redundancy often complicate lightweight solutions to the design problem.

Analytical studies of the early 1970's (refs. 1 to 5) indicate that a solution to the thermal-structural problems associated with stagnation regions of hypersonic aerospace vehicles might be alleviated by the use of heat pipes to cool these regions. Radiant heat and wind tunnel tests of a heat-pipe-cooled wing leading edge designed for a shuttle-type vehicle (refs. 6 to 8) verified the feasibility of heat-pipe cooling for leading edges. Subsequent work (refs. 9 to 12) improved the design and made it lighter and advanced the analytical capability to predict transient and steady-state heat-pipe performance. Recent work on a novel refractory-composite/refractory-metal heat-pipe-cooled leading edge concept for the NASP combines advanced high-temperature materials, coatings, and fabrication techniques with an innovative thermal-structural design. Preliminary design studies (refs. 13-14) indicate that the new leading edge concept can reduce the mass by over 50 percent from an actively cooled design, can completely eliminate the need for active cooling, and can potentially provide failsafe and redundancy features. The present paper reviews the state-of-the-art of heat pipes for cooling wing leading edges of hypersonic vehicles from early application for space-shuttle-type space transportation systems to the present, single-stage-to-orbit NASP.

BRIEF HISTORY OF HIGH-TEMPERATURE HEAT-PIPE
APPLICATIONS AS APPLIED TO LEADING-EDGE COOLING

In the early 1970's, several feasibility studies were performed to assess the application of heat pipes for cooling leading edges and nose caps of hypersonic vehicles (refs. 1-5). NASA Langley Research Center, through a contractual study (ref. 1), analytically verified the viability of heat pipes for cooling stagnation regions of hypersonic vehicles. In 1972, McDonnell Douglas Astronautics Co. (MDAC) compared four space shuttle wing leading edge concepts (ref. 2): a passive carbon-carbon concept, a passive coated-columbium concept, an ablative concept, and a liquid-metal/superalloy heat-pipe-cooled concept. The heat-pipe-cooled concept was determined to be a feasible and durable design concept, but was slightly heavier than the other candidate concepts. In 1973 MDAC fabricated a half-scale shuttle-type heat-pipe-cooled leading edge to verify feasibility of the concept (ref. 4). This model was tested by a series of radiant heat and aerothermal tests at NASA Langley Research Center from 1977 to 1978 (refs. 6-8) to verify heat pipe transient, startup, and steady-state performance. In 1979 MDAC received a follow-on contract to optimize a heat-pipe-cooled wing leading edge for a single-stage-to-orbit vehicle. Results of the follow-on study (ref. 9) indicated that the mass of a shuttle-type heat-pipe-cooled leading edge could be reduced by over 40 percent by use of a more efficient structural design. In 1986 MDAC received a contract to fabricate and build a sodium/superalloy heat-pipe-cooled leading edge component for an advanced shuttle-type vehicle (refs. 10 and 11). This advanced shuttle-type heat pipe was six-feet long and was tested at MDAC by radiant heating (ref. 11) and at Los Alamos National Laboratories by induction heating. NASA has also funded a grant with Georgia Institute of Technology which resulted in the development of a finite element solution for liquid-metal heat-pipe startup from the frozen state (ref. 12).

Recently, NASA Langley has been investigating the use of an advanced heat-pipe-cooled wing leading edge design which is based on high-temperature refractory-composite materials such as carbon-carbon for the structure, refractory-metals such as tungsten or molybdenum for the heat-pipe container, and lithium for the working fluid. The new concept described above is referred to as a refractory-composite/heat-pipe-cooled wing leading edge and is proposed for the wing leading edge of the National Aero-Space Plane (refs. 13 and 14).

The following discussions will summarize significant results of the above mentioned experiments and studies.

Early 1970's	Feasibility studies
1973	Half-scale shuttle-type heat-pipe-cooled wing leading edge (MDAC)
1975-1978	Radiant heat and aerothermal test at LaRC
1979	Follow-on study by MDAC to minimize mass
1985-1988	Finite element solution of startup from the frozen state (Ga. Tech.)
1986	Fabrication of Na/superalloy heat-pipe for wing of advanced STS (MDAC)
1989	Induction heating test of MDAC heat pipe at LANL
1991-present	NASP Government Work Package to design, fabricate, and test refractory-composite/heat-pipe-cooled wing leading edge (LaRC)

Figure 1. - Brief history of high-temperature heat-pipe applications as applied to leading-edge cooling.

PRINCIPLE OF OPERATION OF A HEAT PIPE AS APPLIED TO LEADING EDGE COOLING

A schematic diagram of the general principle of operation of a heat pipe and how it is applied to leading edge cooling is shown in figure 2. A heat pipe is a self-contained, two-phase heat transfer device which is composed of a container, a wick, and a working fluid. Heat input locally to one section of the heat pipe, the evaporator region, is conducted through the container and into the wick/working-fluid matrix, where it is absorbed by the evaporation of the working fluid. The heated vapor flows to a slightly cooler section of the heat pipe where the working fluid condenses and gives up its stored heat. The heat is then conducted through the wick/working-fluid matrix and container and is rejected. The location of the heat pipe where heat is rejected is called the condenser region. The cycle is completed with the return flow of liquid condensate back to the heated region (evaporator) by the capillary pumping action of the wick. During normal operation, heat pipes operate as devices of very high effective thermal conductance and maintain a nearly uniform temperature over the entire heat-pipe length.

Applied to the wing leading edge stagnation heating problem of high-speed aerospace vehicles, heat pipes transport the high net heat input near the stagnation region to cooler aft surfaces, raising the temperature there above the radiation equilibrium temperature and thus rejecting the heat by radiation. The location and extent of the evaporator and condenser regions, which are by definition areas in which there is a net inflow or outflow of heat, respectively, is dependent upon the magnitude and distribution of heating and will vary to satisfy an overall energy balance.
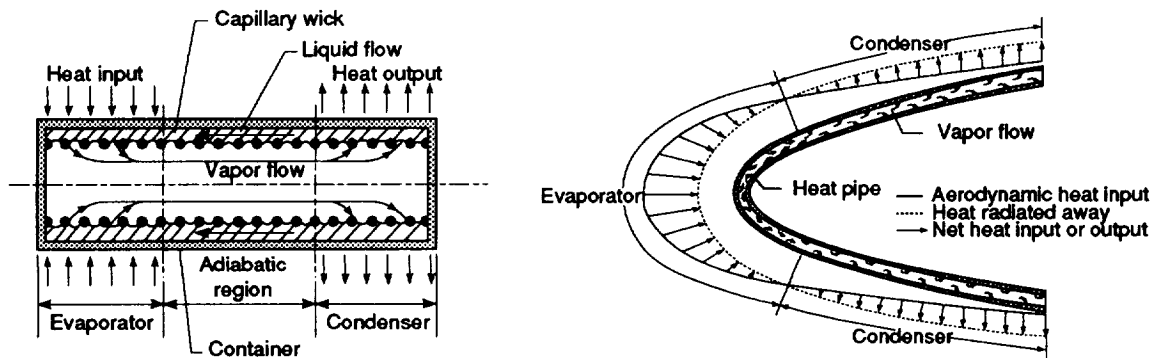
a) Schematic of heat pipe operation   b) Heat pipe cooling applied to leading edge.

Figure 2. - Principle of operation of a heat pipe as applied to leading edge cooling.

HEAT-PIPE HEAT TRANSPORT LIMITS

A given heat pipe can operate over a range of temperatures; however, at each temperature there is a maximum axial heat transport capacity and radial heat flux above which normal heat pipe operation is disrupted. Four such operational limits are shown schematically in figure 3. These limits are the sonic, entrainment, wicking, and boiling limits. The sonic limit usually occurs at low vapor temperatures when the velocity of the vapor can become sonic and the axial heat transport in the heat pipe is limited by a choked-flow condition. During startup of a heat pipe from the frozen state, when the working fluid is solid, the axial heat transfer in the heat pipe is usually limited by sonic flow. Although the sonic limit alone typically does not cause a failure of the heat pipe, it causes the operating temperature of the heat pipe to rise which may cause other limiting conditions to be encountered. The entrainment limit occurs when the drag force of the vapor on the liquid condensate returning to the evaporator is sufficient to overcome the surface tension forces of the liquid within the wick and entrain liquid droplets in the vapor flow. The entrainment of liquid intended to flow to the evaporator region could lead to dryout of the wick in the evaporator region and result in over heating and excessive local temperatures there. The wicking limit is reached when the surface-tension pumping capability of the wick is just sufficient to provide the liquid mass flow rate needed to balance the applied heating rate. Liquid and vapor frictional losses tend to decrease the flow rate of liquid condensate to the evaporator region. Inertial forces caused by vehicle acceleration and gravity can tend to reduce or increase the flow of liquid condensate to the evaporator region. If the wicking limit is exceeded, dryout will occur in the evaporator and result in overheating.

Vaporization of the working fluid normally occurs in the evaporator region of the heat pipe at the liquid-vapor interface. At high radial heat input levels, however, the superheated liquid can reach a critical value at which boiling can occur near the heat pipe wall. The boiling limit is reached when the heating rate is high enough to cause the formation of a continuous vapor film at the heat pipe wall which inhibits the radial flow of heat into the working fluid. The boiling limit is usually not a limiting condition for liquid-metal heat pipes because of the high thermal conductivity of the liquid-metal working fluid and the large amount of superheat needed to initiate boiling.

The boiling limit is a limit on the radial heat flux density, whereas the sonic, entrainment and wicking limits are limits on the axial heat flux density. Further detailed explanations of heat-pipe theory and operating limit calculations can be found in references 15 and 16.
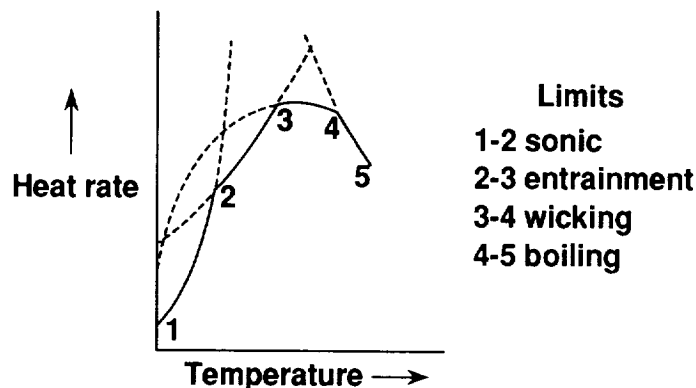

Figure 3. - Heat transport limits.

SHUTTLE-TYPE HEAT-PIPE-COOLED WING
LEADING EDGE TEST MODEL

A one-half scale heat-pipe-cooled wing leading edge test model fabricated by MDAC for a shuttle-type vehicle and trajectory is shown in figure 4. The test model is six-inches in span, has a chord length of 22 in., and is 13-in. high at its base. It consists of 12 sodium-charged heat pipes which are brazed to each other and to the inner surface of a thin (0.02-in.-thick) Hastelloy-X skin. The heat pipes are Hastelloy-X circular cylinders which have an outer diameter of 0.5 in., a wall thickness of 0.05 in., and a wick thickness of 0.035 in. The wick consists of seven alternate layers of 100- and 200-mesh stainless-steel screen and is a concentric annulus design. The heat pipes are sized so that one heat pipe could become inoperative without compromising structural integrity, thus providing a fail-safe capability. The skin is coated externally with a high-emissivity ceramic paint to facilitate heat rejection by radiation.
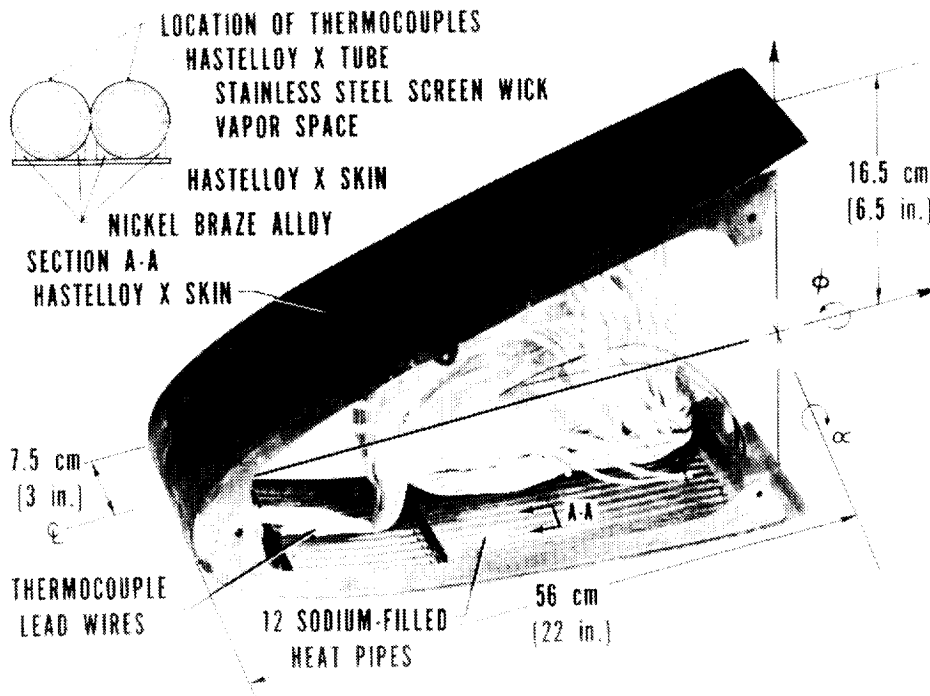

Figure 4. - Shuttle-type heat-pipe-cooled wing leading edge test model.

SHUTTLE-TYPE HEAT-PIPE-COOLED WING LEADING EDGE DURING A RADIANT HEAT TEST

Performance of the shuttle-type heat-pipe-cooled wing leading edge was studied by a series of radiant heat and aerothermal tests. The purpose of the radiant heat tests was to investigate heat-pipe startup from the frozen state (working fluid initially frozen or solid), and transient and steady-state thermal performance of the leading edge test model. For the radiant heat tests (fig. 5), angle of attack, α, was simulated by orienting the model at the angle α with respect to the horizontal to obtain the desired gravity effect and by positioning three radiant heaters about the model to provide a heating distribution representative of the aerodynamic heating distribution at that angle. Three water-cooled calorimeter gages were used, one in each of three separate feedback control loops, to regulate output of each lamp bank separately. Power to the lamp banks was varied to simulate a shuttle reentry heating trajectory. The test model was subjected to a total of seven radiant heat tests with cold-wall heating rates ranging from 21.1 to 34.8 Btu/ft^2-s, angles of attack ranging from 0 to 20 degrees, and maximum surface temperatures ranging from 1130 °F to 1380 °F. Details of the radiant heating tests can be found in reference 6.
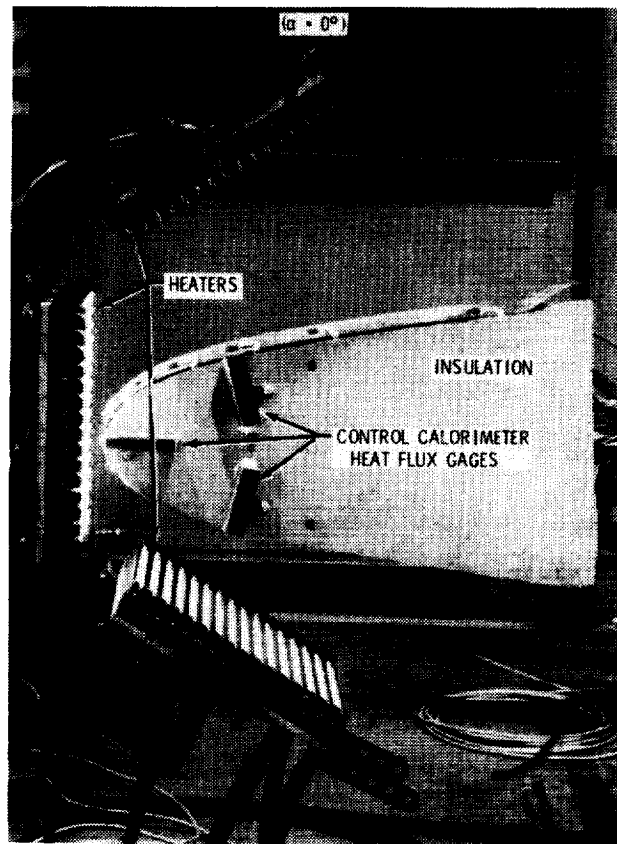

Figure 5. - Shuttle-type heat-pipe-cooled wing leading edge during a radiant heat test.

WIND TUNNEL CONFIGURATION OF HEAT-PIPE-COOLED WING LEADING EDGE

After completion of the radiant heat tests, the heat-pipe-cooled leading edge was fitted with spanwise extensions and aerodynamic fences (fig. 6) for aerothermal testing in the Langley 8-Foot High Temperature Tunnel. The purpose of the extensions and fences was to produce a two-dimensional flow field over the test model and to allow measurement of flow conditions over the leading edge. The purpose of the aerothermal tests was to investigate performance of the model subject to realistic aerothermal loads. To avoid unrealistically severe heat pulses and to insure proper startup of the heat pipe, the model was preheated prior to insertion into the test stream. A simple heater array was used to preheat the model; no attempt was made to simulate an aerodynamic heating distribution during preheating. The model withstood 27 supplemental radiant heat cycles lasting 30 minutes each during which the maximum surface temperatures ranged from 1100 °F to 1480 °F. Cold-wall stagnation heating rates ranged from 21.1 to 34.8 Btu/ft^2-s for the radiant preheating cycles and hot-wall stagnation heating rates ranged from 21.5 to 37.2 Btu/ft^2-s for the aerothermal tests. The maximum cold-wall heating rate of the aerothermal tests was 56.9 Btu/ft^2-s and maximum heat-pipe operating temperatures ranged from 1090 °F to 1520 °F. The model was subjected to a total of eight aerothermal tests with angle of attack variations of 0-, 10-, and 20-degrees; and roll variations of 0- and 90-degrees. The 90-degree roll condition was included to investigate the effect of gravity on heat-pipe performance.

The heat pipes operated isothermally for these test conditions with maximum operating temperatures ranging from 1250 to 1520 °F. Near steady-state temperatures obtained during the aerothermal tests were in good agreement with analytical results. The pressure and heat-flux distributions were also in good agreement with design distributions.
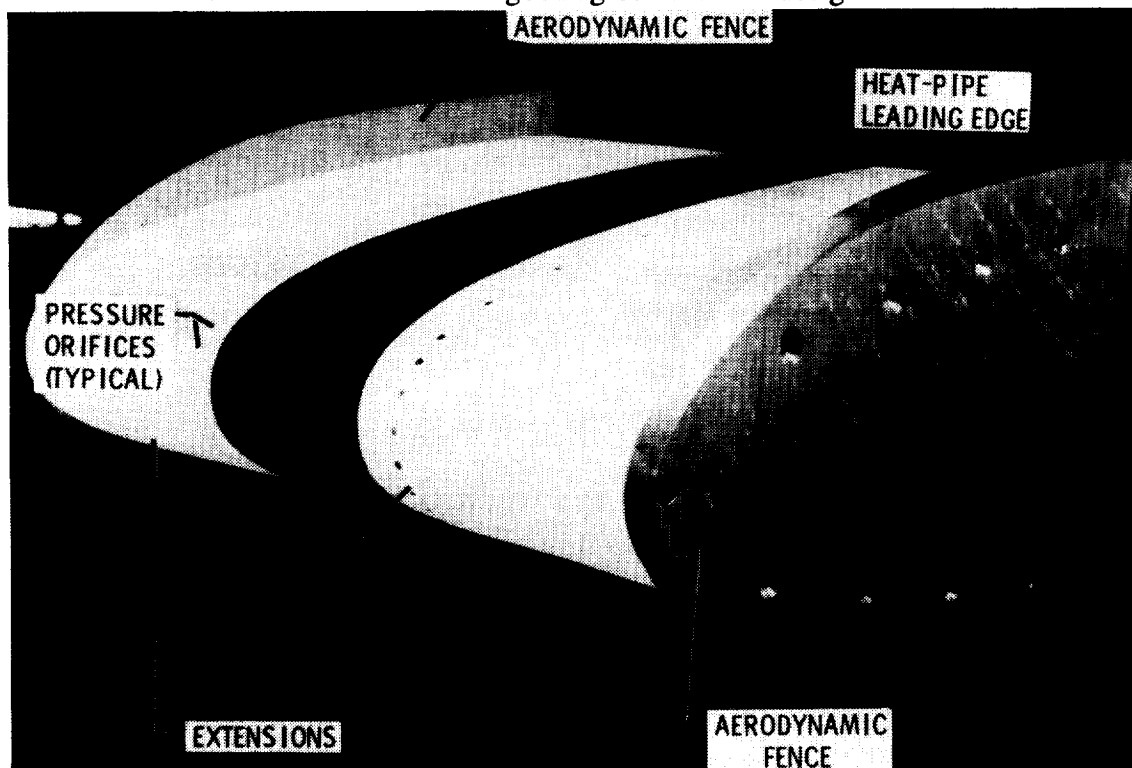

Figure 6. - Wind tunnel configuration of heat-pipe-cooled wing leading edge.

SIMPLIFIED MODEL OF TRANSIENT HEAT-PIPE STARTUP FROM THE FROZEN STATE

A schematic diagram of the simplified analysis model used to predict the heat-pipe startup, transient, and steady-state response is shown in figure 7. The simplified analysis assumes the momentum and energy equations are uncoupled and solves for heat pipe temperatures directly from an energy balance. The analysis method used is similar to that of reference 17 and assumes the initial temperature of the heat pipes is below the melting point of the working fluid and, consequently, the working fluid is in the frozen or solid state and the vapor pressure is low. Thus, free molecular flow conditions exist throughout the heat pipe and axial heat transfer is very low. As heat is applied, the temperature and vapor pressure of the most highly heated region increases until continuum flow conditions are established and the heat pipe begins to operate locally in that region. Additional heating causes the temperature of the continuum region to increase and the continuum front to extend into adjacent free molecular flow regions.

An aerodynamic heating distribution was approximated by six constant heat input regions as shown in figure 8. Continuum flow initiates in the region of highest heat input and is assumed to occur when the molecular mean free path of the sodium vapor is equal to or less than 0.01 times the diameter of the vapor space. During startup, axial heat transport, $\dot{Q}_a$, is assumed to occur from continuum flow regions at the sonic heat transport limit and all heat is assumed to be rejected by radiation, $\dot{Q}_r$. An effective volumetric heat capacity per unit heat-pipe length, C, was calculated as a function of temperature and was used in simple energy balances to determine continuum and free molecular region temperatures and to determine continuum region growth.
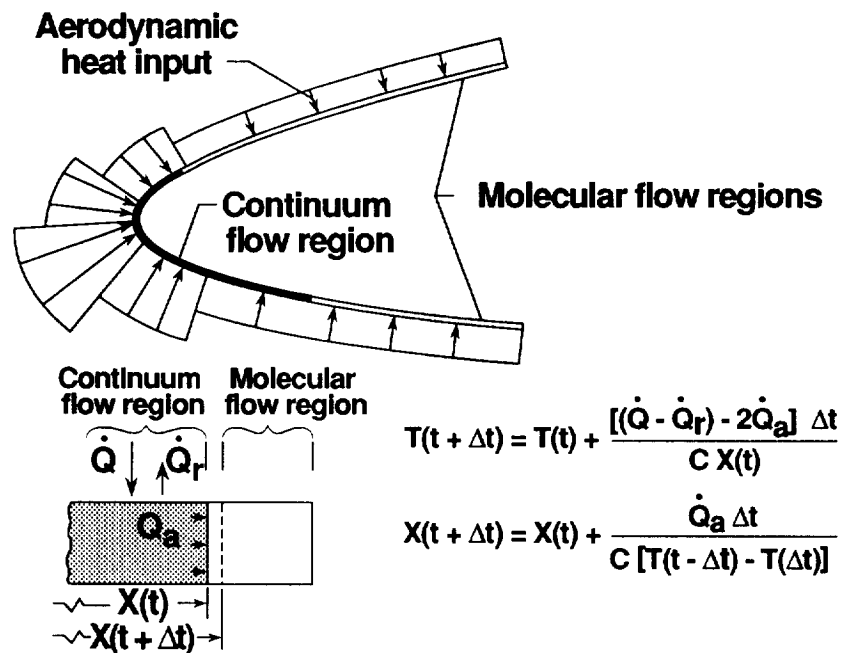

$$T(t + \Delta t) = T(t) + \frac{[(\dot{Q} - \dot{Q}_r) - 2\dot{Q}_a] \, \Delta t}{C \, X(t)}$$

$$X(t + \Delta t) = X(t) + \frac{\dot{Q}_a \, \Delta t}{C \, [T(t - \Delta t) - T(\Delta t)]}$$

Figure 7. - Simplified model of transient heat-pipe startup from the frozen state.

298

RESULTS OF REENTRY SIMULATION TEST USING RADIANT HEATERS

Results of a radiant heating test which simulates a shuttle-type reentry heating trajectory are shown in figure 8. Experimental and analytical temperature histories at three locations along the upper surface of the leading edge agree except for times greater than 800 seconds at which point calculated temperatures are approximately 150 °F greater than experimental values. The lower than expected experimental temperatures are believed to be caused by heat lost by free convection during the experiment which was not accounted for in the analysis. The sharp rise in temperature at the onset of heating occurs because axial heat transport is low since free molecular flow conditions prevail in the vapor space. Hence, temperatures in the aft region ($\ell/\ell_T = 0.88$), for instance, rise slowly. When the continuum vapor front propagates to the aft region (at approximately time t = 600 seconds), the temperature there rises very rapidly to the continuum flow region temperature as shown in figure 8. No startup problems were encountered and the heat pipes became fully operational at t = 700 seconds and a temperature of about 1200 °F.
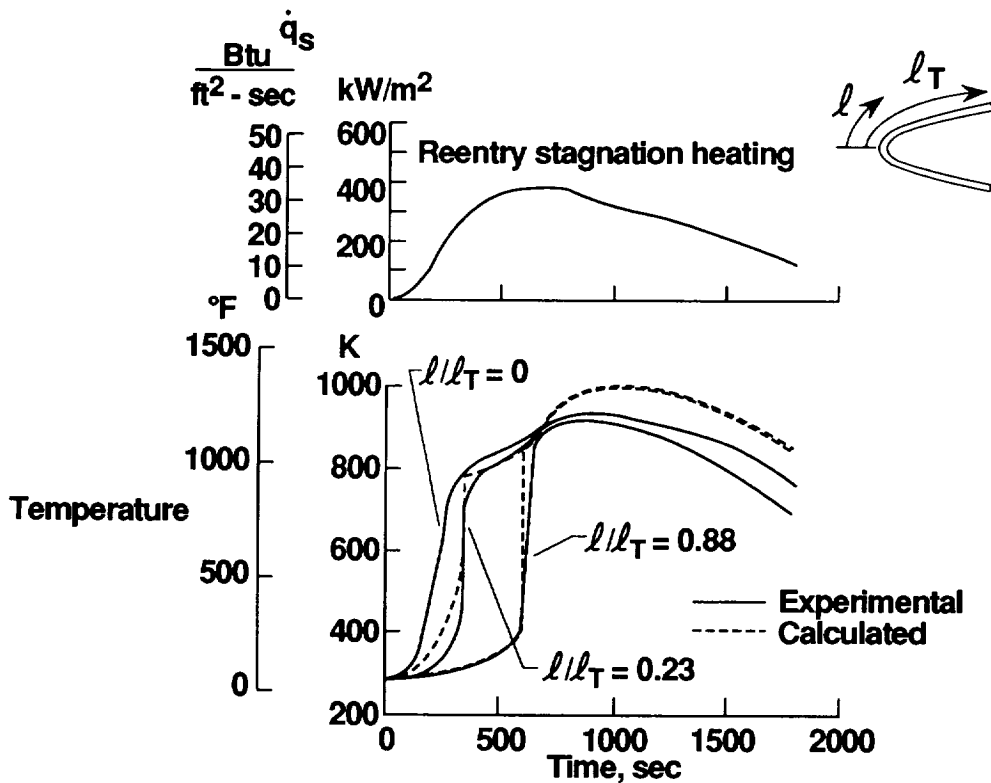

Figure 8. - Results of reentry simulation test using radiant heaters.

TEMPERATURE DISTRIBUTIONS DURING TRANSIENT HEAT-PIPE STARTUP

Temperature distributions along the lower and upper surfaces of the leading edge during three different phases of heat-pipe startup (unstarted, starting, and fully operational) are shown in figure 9 for a zero-degree angle-of-attack test ($\alpha = 0°$). In the unstarted state, the working fluid is frozen and, hence, the temperature distribution is similar to that of an uncooled leading edge (i.e., high local temperatures near the locally heated nose region and a rapid drop in temperatures away from the nose region). Once continuum flow occurs, the heat pipe is partially started and there exists a local continuum flow region where temperatures are nearly uniform. Located next to the continuum flow region are two free molecular flow regions where axial heat transfer is low and large axial temperature gradients exist. Once the continuum flow region propagates to the extreme ends of the heat pipes, the heat pipes are assumed to be fully operational and nearly isothermal as shown in figure 9.

Although startup and transient heat pipe operation has been predicted with reasonable accuracy using simplified mathematical models, more work is necessary to predict accurately the transient heat-pipe operating limits. Slight variations in heat-pipe temperature and pressure can produce large variations in predicted operating limits and, hence, improved analytical methods are necessary. Finite element and finite difference methods can be used to solve the coupled momentum and energy equations and incorporate working fluid phase change, compressible fluid flow, and three-dimensional heat transfer.
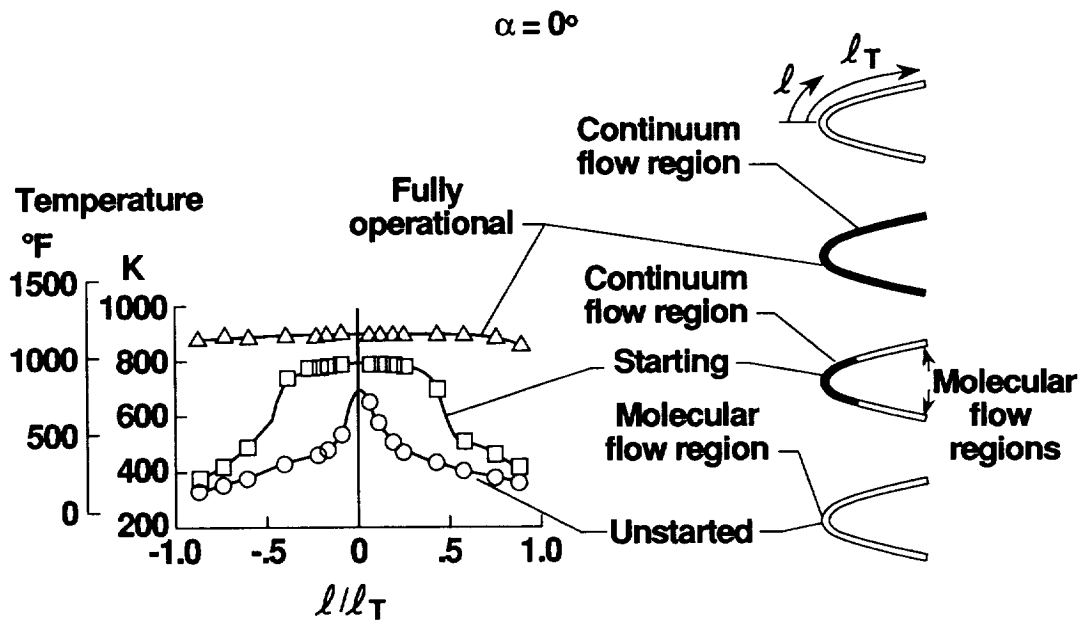

Figure 9. - Temperature distributions during transient heat-pipe startup.

THERMAL BUCKLING OF HEAT-PIPE-COOLED WING LEADING EDGE

Results of the aerothermal tests dramatically demonstrate the durability of the heat pipe leading edge. The initial configuration of the radiant heaters for the preheating of the model caused a wicking limit to occur prior to the first aerothermal test. The encounter with the wicking limit caused a wick dryout condition to occur locally in the upper aft region of the leading edge due to the location of the heaters. During this dryout condition, local temperatures exceeded 1900 °F. The high local temperatures, coupled with the constraint imposed by the side extensions in the lateral directions, caused local buckling of the aerodynamic skin in regions between the cylindrical heat pipes as shown in figure 10. However, the structural integrity of the test model was not severely compromised as demonstrated by the successful completion of the remaining six aerothermal tests.
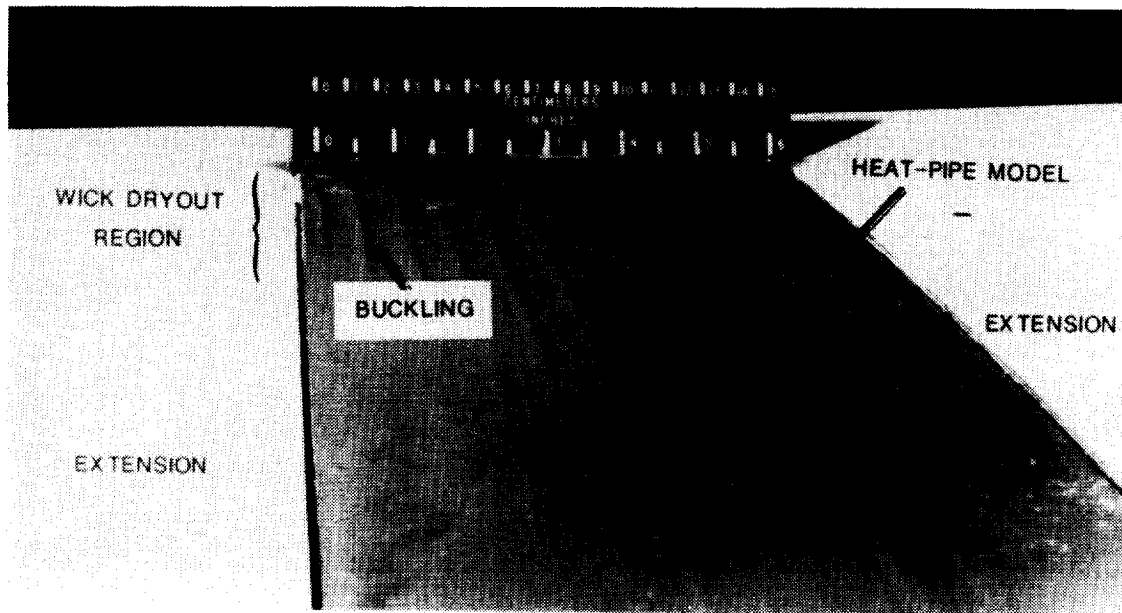

Figure 10. - Thermal buckling of heat-pipe-cooled wing leading edge.

EROSION DAMAGE OF HEAT-PIPE-COOLED WING LEADING EDGE

Debris in the test stream of the Eight-Foot High Temperature Tunnel (tests were performed prior to tunnel modification which reduced the debris threat) caused some erosion damage to the model as shown in figure 11. After two aerothermal tests, the nose region of the heat-pipe leading edge model was pitted and the zirconium coating on the stainless-steel water-cooled extensions was severely eroded. The thin Hastelloy-X skin (0.02-in. thick) suffered minor damage but no particle penetration. However, the high emissivity ceramic paint eroded near the nose and exposed the metal surface to oxidation by the airstream.
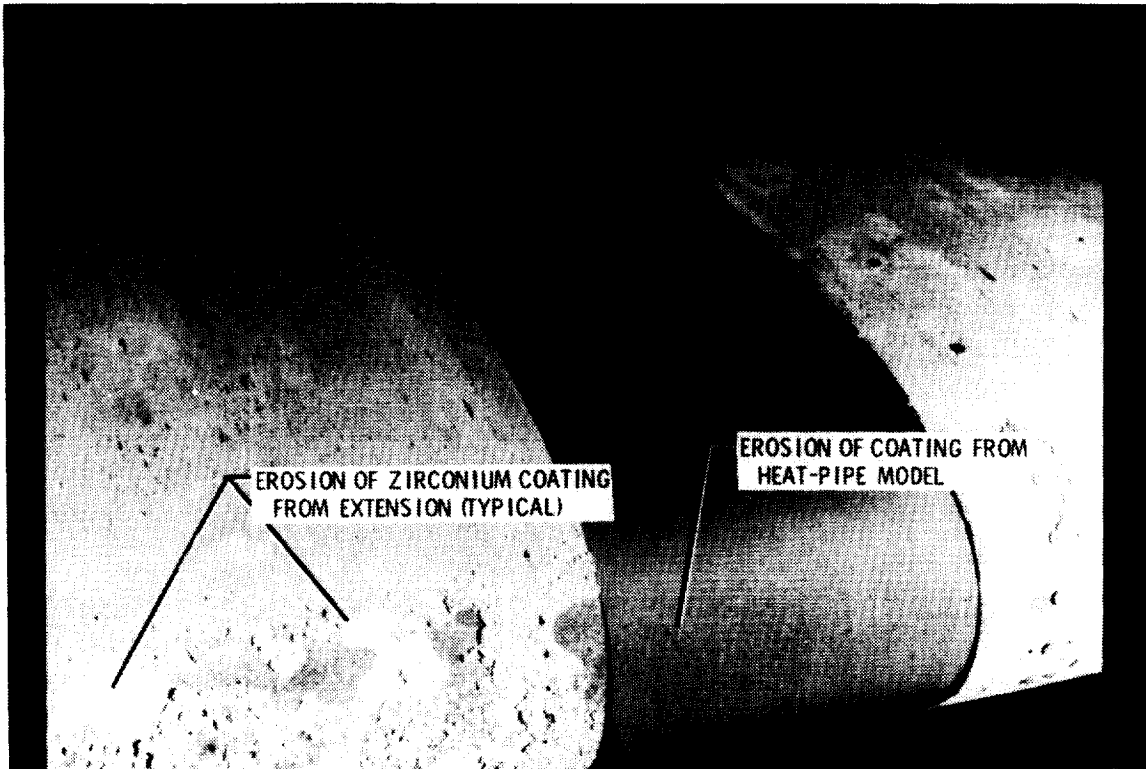

Figure 11. - Erosion damage of heat-pipe-cooled wing leading edge.

DEVELOPMENT OF NUMERICAL METHOD FOR PREDICTING TRANSIENT HEAT-PIPE OPERATION FROM THE FROZEN STATE USING FINITE ELEMENT ANALYSIS

A finite element analysis code has been developed which solves the coupled thermal-fluid heat pipe problem and is capable of accurately predicting heat-pipe temperatures and temperature gradients as well as liquid and vapor pressures and velocities. Numerical results for startup of a liquid-metal heat pipe subject to a typical aerodynamic heat input and representative of a radiant-heat test of a shuttle-type heat-pipe-cooled leading edge are shown in figure 12, and the results compare well with experimental results (refs. 6-8).

Since a typical aerodynamic heating distribution was approximated for both the experimental and numerical cases, the heat input at the stagnation region was much greater than in the aft regions. As expected, the temperatures began to rise in the stagnation region sooner than in the aft regions, resulting in a large temperature gradient in the heat pipe during start-up. For about the first 450 seconds, the heat pipe is not operational as the vapor density is still quite small. After 550 seconds, the vapor flow has transitioned from free molecular flow to continuum flow, and an isothermal region can be observed in the stagnation region, while most of the rest of the heat pipe is still at the initial temperature. The region of continuum flow continues to increase and becomes isothermal near a time of 1200 seconds. However, the temperature of the heat pipe continues to increase until a steady-state value is reached at a later time.
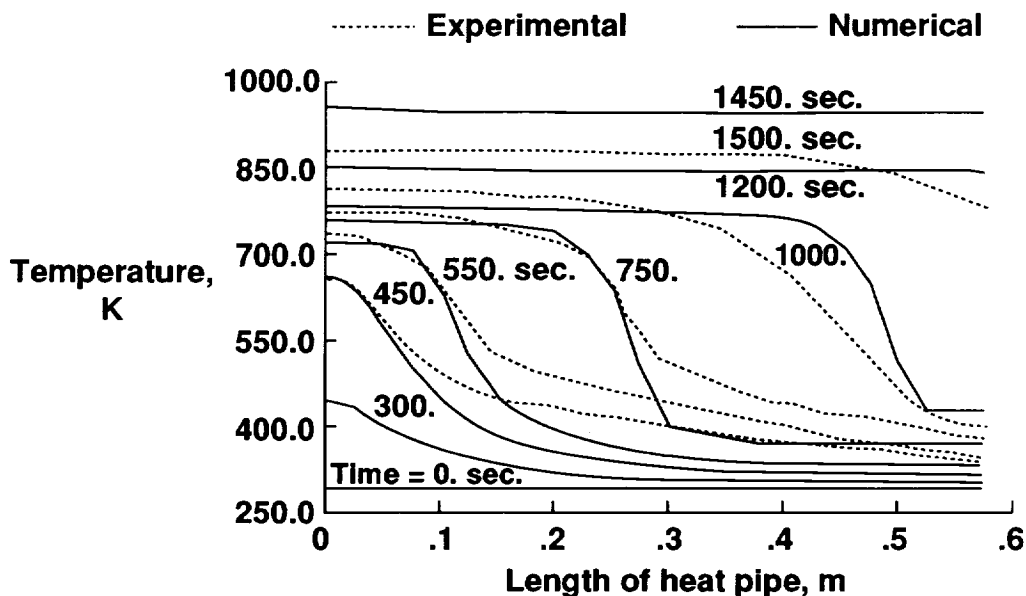

Figure 12. - Comparison of numerical and experimental temperature distributions in a heat-pipe-cooled leading edge during startup from the frozen state.

IMPROVED HEAT-PIPE DESIGN

A follow-on study contract was awarded to MDAC (NASA Contract NAS1-15554) to investigate thermostructural applications of heat pipes (ref. 9). A heat-pipe-cooled leading edge was designed for a single-stage-to-orbit vehicle and optimized with respect to mass to make it competitive with carbon-carbon and refractory-metal versions of the leading edge. The improved design, shown in figure 13, uses a Hastelloy-X D-tube corrugated section which is seam welded to a thin Hastelloy-X facesheet. The new configuration eliminates the need for the braze fillets of the cylindrical tube design (used to enhance heat conduction into the heat pipe) and reduces mass by approximately 44 percent compared to a design which uses circular cylindrical tubes brazed to a thin facesheet.
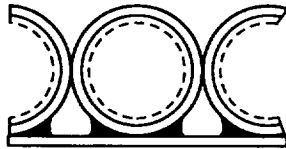
3.4 lb/ft² - Not competitive with carbon-carbon

1.9 lb/ft² - Competitive with carbon-carbon

Figure 13. - Improved heat pipe design.

HEAT-PIPE-COOLED WING LEADING EDGE DESIGN FOR AN ADVANCED SPACE TRANSPORTATION SYSTEM

A sodium/Hastelloy-X heat pipe was designed for use in the leading edge of an advanced space transportation system (refs. 10-11) and a single full-scale heat pipe was fabricated for testing. A schematic diagram of the heat pipe for the wing of an advanced shuttle-type vehicle is shown in figure 14. The heat pipe was designed to be oriented normal to the leading edge. Aft of the heat pipe, more conventional hot structure designs, for example, carbon-carbon, were assumed on the lower surface. The heat pipe is intended to reduce maximum wing leading edge temperatures during re-entry from 3500 °F to 1800 °F. The total length of the heat pipe necessary to radiate enough heat to reduce maximum temperatures to 1800 °F was determined from an energy balance over the entire heat pipe. A large angle of attack during re-entry would result in higher heat loads on the lower surface, thus providing a considerable heat sink on the upper surface. The heat pipe length on the lower surface was sized such that the radiation equilibrium temperature of the region beyond the end of the heat pipe was less than 2800 °F. This sizing operation resulted in a total heat pipe length of 69 in., with 3 in. of that on the lower surface.

The Hastelloy-X heat-pipe container had a rectangular cross section and a stainless steel wick which was diffusion bonded to the inner surface of the container. A 0.030-in.-thick "U-shaped" channel and a 0.060-in.-thick flat strip with a 0.030-in. step milled in its edges made up the heat pipe components. In the evaporator region, two layers of 50-mesh stainless-steel screen were placed between two layers of 200-mesh screen on the heated surface, while two layers of 200-mesh screen were used on the side walls. No screen was placed on the back wall in the evaporator region. In the condensor region, eight layers of 50-mesh screen were placed between two layers of 200-mesh screen on the heated surface, and two layers of 200-mesh screen were used on the other three walls. The purpose of the composite wick (50-mesh screen between 200-mesh screen) was to achieve the high capillary pressure provided by the 200-mesh screen and the high permeability of the 50-mesh screen.

The heat pipe was instrumented with internal pressure transducers and external thermocouples. Graphite heaters were used to heat the heat pipe during the tests. A burn-through of the heat pipe container occurred in the stagnation region during the second test. Post test X-rays indicated that the sodium working fluid had not been evenly distributed in the wick prior to testing. A second heat pipe was then assembled at Los Alamos National Laboratory (LANL) with spare parts which remained after fabrication of the first heat pipe. Tests were conducted to determine the basic performance limits of the heat pipe.
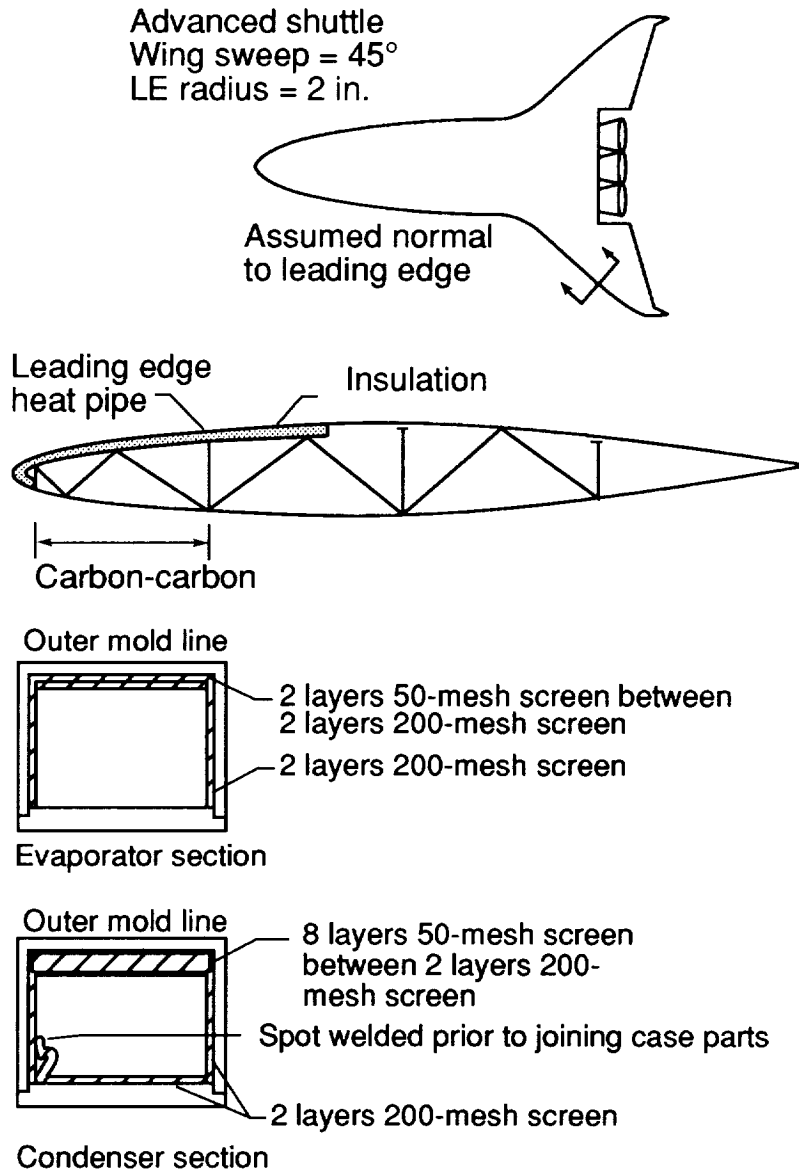
Advanced shuttle
Wing sweep = 45°
LE radius = 2 in.

Assumed normal
to leading edge

Leading edge
heat pipe   Insulation

Carbon-carbon

Outer mold line

2 layers 50-mesh screen between
2 layers 200-mesh screen

2 layers 200-mesh screen

Evaporator section

Outer mold line

8 layers 50-mesh screen
between 2 layers 200-
mesh screen

Spot welded prior to joining case parts

2 layers 200-mesh screen

Condenser section

Figure 14. - Heat-pipe-cooled wing leading edge design for an advanced space transportation system.

306

SIX-FOOT-LONG HASTELLOY-X/SODIUM HEAT PIPE DURING INDUCTION HEATING TEST AT LOS ALAMOS NATIONAL LABORATORY

A radio frequency (RF) induction heating device was used for all of the testing of the Hastelloy-X/sodium heat pipe. To simulate the wing leading edge heating, a shaped RF induction concentrator was used. A mica sheet was attached to the heat pipe to insulate electrically the heat pipe from the RF concentrator. The specially designed heat source provided a stagnation zone heat input over the outside surface of the evaporator region of the heat pipe. The heat pipe was instrumented with eight thermocouples which were spot welded to the external surface. Thermocouples were attached to the middle of the evaporator and each end of the evaporator section, and five equally spaced thermocouples were located in the condenser section.

Several start-up tests of the heat pipe were conducted. It was found that the heat pipe was extremely sensitive to transients, both during and after start-up. A photograph of the heat pipe during steady state operation is shown in figure 15. It was observed that insulating three sides of the condenser assisted in both the start-up and steady-state operation of the heat pipe. The insulation reduced the axial thermal load on the heat pipe, and thus reduced the pumping requirements of the wick. Post test permeability analyses revealed that the composite wick, using a 200-mesh screen at the liquid vapor interface for high capillary pressures, did not provide the required pumping pressure. The inability to generate the required pumping pressures was probably due to a breach in the 200-mesh screen. With a tear in the 200-mesh screen, the maximum pumping pressures that could be generated resulted from the 50-mesh screen which was located next to the 200-mesh screen. Estimates of the capillary size which would cause a wicking limit to occur during the induction heating test are consistent with a 50-mesh screen and, thus tend to verify that a breach in the 200-mesh screen had occurred.
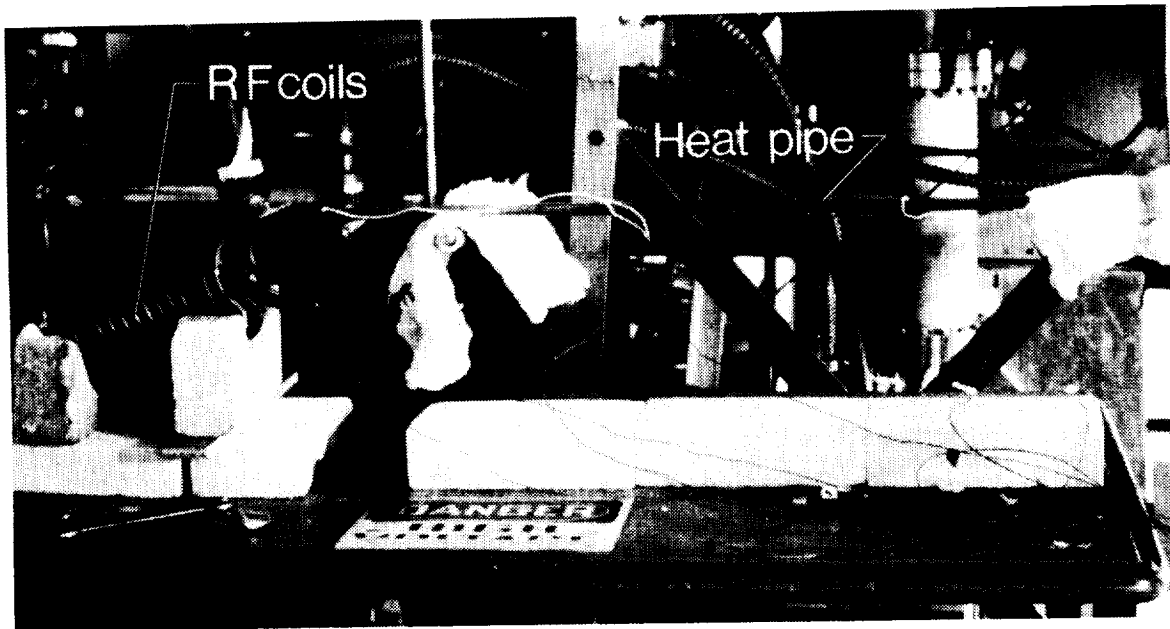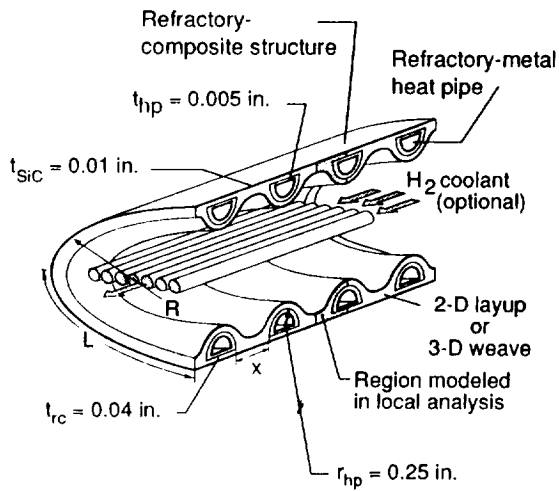

Figure 15. - Six-foot-long Hastelloy-X/sodium heat pipe during induction heating test at Los Alamos National Laboratory.

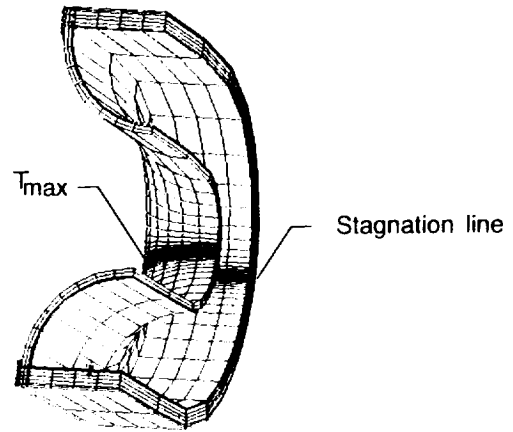# HEAT-PIPE-COOLED WING LEADING EDGE FOR THE NATIONAL AERO-SPACE PLANE

Heat pipes are being considered for use on the wing leading edge of the NASP. The concept being considered has refractory-metal heat pipes embedded in a refractory-composite structure. The refractory-composite structure is protected from oxidation by a thin layer of silicon carbide (SiC). If external radiative cooling to space is inadequate to reduce effectively the leading edge temperatures, additional radiative cooling to a heat exchanger, located inside the wing leading edge, may be used. Hydrogen fuel would be used for a coolant in the heat exchanger.

A schematic diagram of the heat-pipe-cooled wing leading edge for NASP is shown in figure 16. A region of both the upper and the lower surface of the leading edge is shaded to represent the region modeled in the finite element analysis. Since the maximum leading edge temperatures occur midway between heat pipes in the stagnation region, a simplified 1-D or 2-D analysis cannot adequately model the leading edge temperatures. Thus, a 3-D finite-element analysis was used for the thermal parametric study. Two different boundary conditions were considered for the interior of the leading edge: one for internal radiative cooling (cooled), and the other for a surface with no internal radiative cooling (uncooled). Thermal effects of both the 2-D layup and the 3-D woven refractory composite architectures were considered, and different refractory metals were considered for the heat pipe container. The heat pipe wall thickness, t_{hp}, remained constant at 0.005 in., the SiC coating thickness, t_{SiC}, remained constant at 0.010 in., the refractory-composite thickness, t_{rc}, remained constant at 0.040 in., and the semicircular heat-pipe cross-sectional radius, r_{hp}, remained constant at 0.25 in. The leading edge radius, heat-pipe length, and heat-pipe spacing were varied in the parametric analysis.

The Engineering Analysis Language (EAL) system (ref. 18) was used for the finite-element analysis. A parametric model was constructed using the Execution Control System language in EAL which enabled the physical dimensions of the leading edge, the refractory-composite and heat-pipe material properties, and the boundary conditions to be varied easily. The forward portion of the finite element model shown on the right hand side of figure 16 represents a leading edge with a 0.5-in. radius, and the lengths of the upper and lower surfaces have been reduced to 0.5 in. to allow all the elements to be included in the illustration. Elements are concentrated in the stagnation region where the temperature and heat flux gradients are the largest. Temperature dependent material properties are used throughout the analysis.

Refractory-
composite structure

Refractory-metal
heat pipe

t_{hp} = 0.005 in.

t_{SiC} = 0.01 in.

H_2 coolant
(optional)

T_{max}

Stagnation line

R

L

x

2-D layup
or
3-D weave

Region modeled
in local analysis

t_{rc} = 0.04 in.

r_{hp} = 0.25 in.

Temperature dependent properties

Thermal analysis: 4500 elements
Structural analysis: 14000 elements

**PARAMETERS USED IN FINITE
ELEMENT MODEL**

FINITE ELEMENT MODEL

Figure 16. - Heat-pipe-cooled wing leading edge for the National Aero-Space Plane.

THERMAL FINITE ELEMENT ANALYSIS OF HEAT-PIPE-COOLED WING LEADING EDGE FOR NASP

The thermal finite element model and the parameters varied in the design study are shown in figure 17. The choice of refractory metals has been shown to have little effect on the maximum leading edge temperatures. In addition, the through-the-thickness thermal conductivity of 2-D advanced carbon-carbon (ACC) material is very low and has been shown to result in excessively high temperatures. As a result, a tungsten (W) heat pipe embedded in 3-D carbon/silicon-carbide (C/SiC) material is considered as a baseline for a series of parametric studies which follow. In each case, heat pipes are considered to extend from a given location on the bottom surface of the leading edge, around the stagnation region and for the same distance along the top surface of the leading edge. The heat pipe is assumed to have a "D-shaped" cross section, with an internal radius of 0.25 in. The parameters that have a significant effect on the maximum leading edge temperatures are the internal boundary condition (cooled or uncooled), the heat-pipe length, the distance between heat pipes, and the leading edge radius. The effect of the heat-pipe length, distance between heat pipes, and internal boundary condition on maximum leading edge temperatures are evaluated.

The maximum leading edge temperature is shown in figure 17 as a function of the heat pipe length (12 in. $\leq L \leq$ 36 in.), the distance between heat pipes (0.02 in. $\leq x \leq$ 0.20 in.) and the internal boundary condition (insulated and radiatively cooled (labeled uncooled and cooled, respectively, in the figure)). As expected, the maximum leading edge temperature increases with increasing distance between heat pipes. The maximum temperature decreases with increasing heat pipe length. This decrease in temperature results from an increase in the surface area that is at high temperature, and thus an increase in radiative heat losses. It is desirable to develop a passive design with no active hydrogen cooling. The heat-pipe-cooled leading edge concept enables a passive design for the assumed NASP heat flux distribution. Though the actively cooled designs result in temperatures below 3000 °F for even a 12-in.-long heat pipe with 0.20 in. between heat pipes, the active cooling provides a weight penalty such that longer heat pipes spaced closer together with no internal cooling is a more favorable design. As a result, an insulated design is chosen as the baseline. An uncooled leading edge with 30-in.-long heat pipes can maintain maximum temperatures below 2765 °F. The heat pipe operating temperature for this case is 2197 °F. Thus, the baseline design includes 30-in.-long heat pipes embedded in C/SiC, with heat pipes spaced 0.06 in. apart. Internal cooling is not used in the baseline design and the baseline design is represented by the large circular symbol in figure 17.
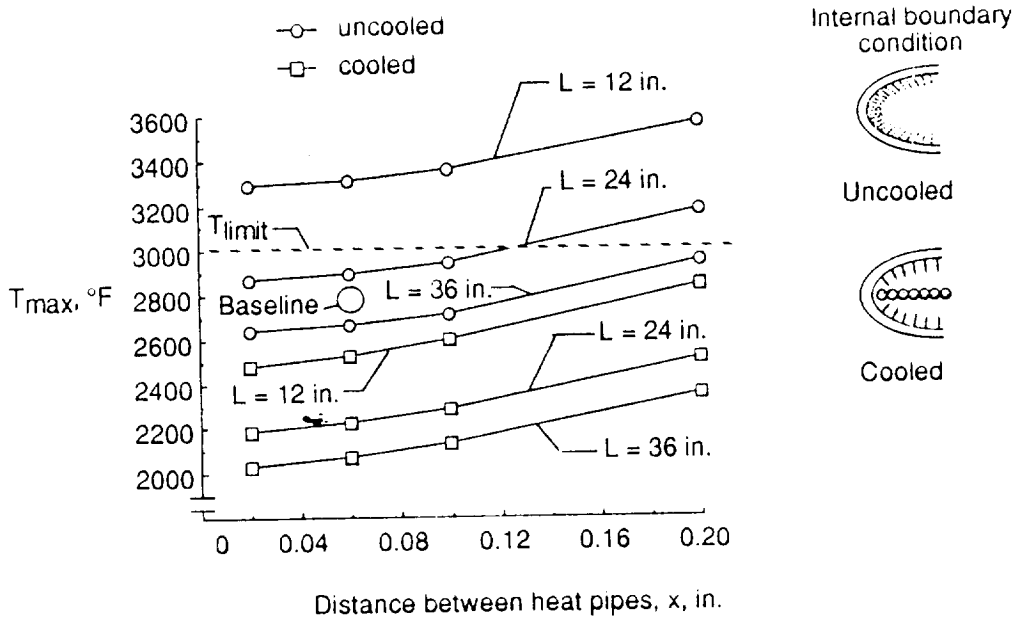
Figure 17. - Thermal finite element analysis of heat-pipe-cooled wing leading edge for NASP.

THERMAL/STRUCTURAL ANALYSIS OF HEAT-PIPE-COOLED WING LEADING EDGE FOR NASP

The finite element analysis used for the thermal parametric study was also used for the thermal-structural analysis. However, a much more refined mesh was used in the thermal-structural analysis than in the thermal analysis alone. The refractory-metal heat-pipe container material considered was molybdenum-47 wt.% rhenium (Mo-47Re) alloy. A 1-in. leading-edge radius was assumed. The thermal stresses in the chordwise direction for a Mo-47Re heat pipe embedded in a C/SiC leading edge are shown in figure 18. Chordwise normal stresses in the thin refractory-metal heat-pipe container material are compressive and quite high. The compressive stresses are higher than the proportional limit for the Mo-47Re at elevated temperature and stress relief by plastic deformation is expected. There are several reasons for the excessively large calculated stresses. The primary reason for the large stresses in the chordwise direction is that the finite element analysis is not able to account for slippage of the heat pipes in the composite structure. Slippage is expected because of the coefficient-of-thermal-expansion mismatch between the refractory-metal and the refractory-composite materials and the lack of sufficient bond strength between the materials. In addition, the analysis is linear and cannot adequately represent the nonlinear behavior of the materials.

Since the refractory-composite material is more brittle than the refractory-metal material and has very low through-the-thickness strength, it is believed that the principal mode of failure will be by cracking of the refractory-composite structure between adjacent heat pipes. This type of problem at elevated temperatures has been experienced previously with cracking of ceramic material with metallic inclusions. Researchers at Thermo Electron Corporation (refs. 19-20) alleviated thermal cracking in the SiC coating of a refractory-metal heat pipe by including a soft carbon middle layer which served as a means for strain isolation. In addition, researchers at General Dynamics were able to embed successfully refractory-metal tubes within C/SiC material (refs. 21-22) and develop an advanced actively cooled panel by tailoring the carbon-fiber preform to minimize the thermal expansion mismatch.
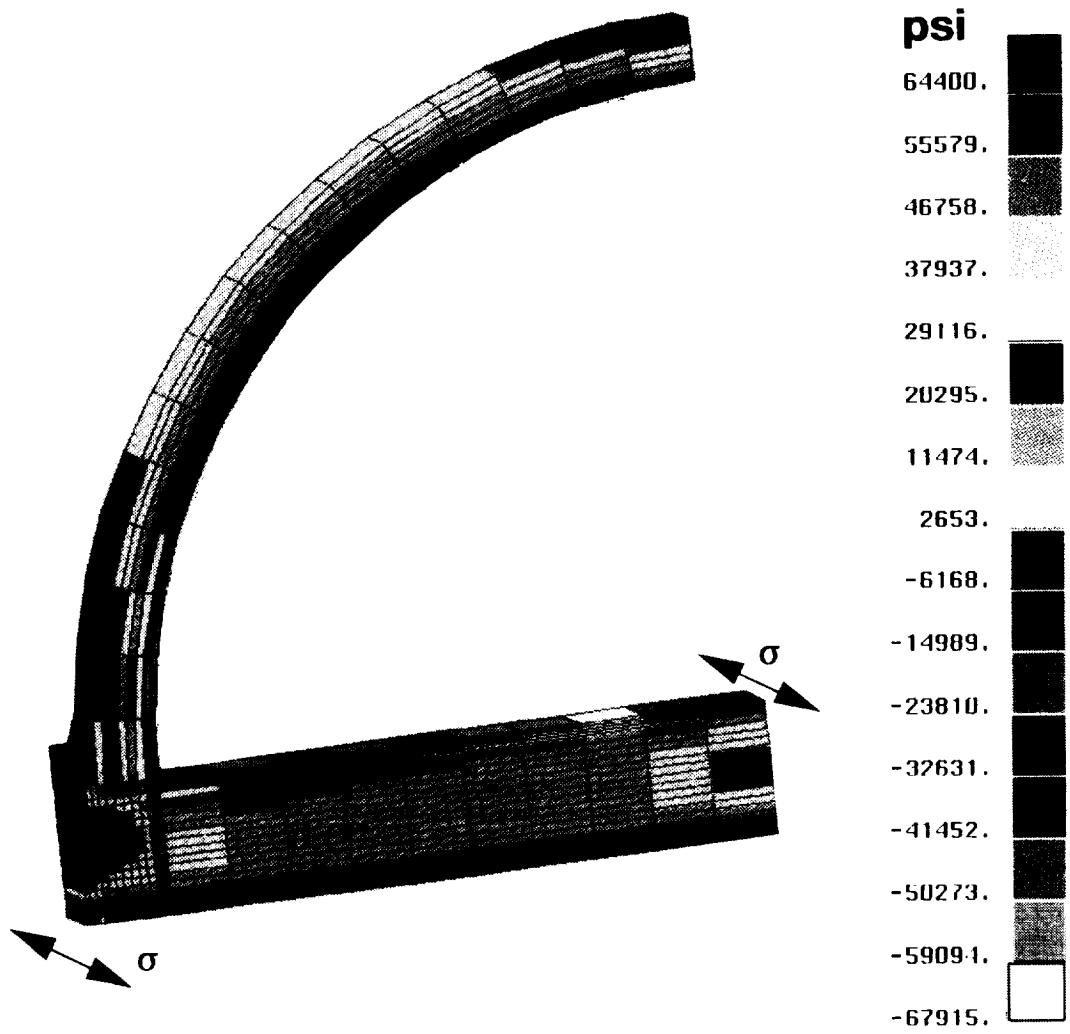
Figure 18. - Thermal/structural analysis of heat-pipe-cooled wing leading edge for NASP.

HEAT PIPE FABRICATION

The first step in the fabrication of the refractory-composite/heat-pipe-cooled leading edge for NASP is the fabrication of curved "D-shaped" refractory-metal tubes. "D-shaped" molybdenum tubes have been drawn by Tecomet Corporation. An attempt has been made to bend a 6-in.-long Mo "D-shaped" tube at Los Alamos National Laboratory (LANL). The tube was successfully bent at an elevated temperature. However, crimping of the tube occurred on the curved, inner portion of the tube, as shown in the top photograph of figure 19. Further attempts will be made to develop a procedure to bend the tubes and eliminate crimping of the inner surface. A screen wick will be used to pump the working fluid from the condenser to the evaporator. A photograph of the screen wick inserted in a Mo "D-shaped" tube is shown in the bottom photograph of figure 19. The wick is made up of three layers of 400-mesh Mo-41Re screen. A 0.1-in.-diameter artery can also be seen in the photograph. The purpose of the artery is to aid in the pumping of the working fluid with a minimum pressure loss.

Initially, "D-shaped" Mo tubes were drawn. However, due to ductility requirements at room temperature, Mo-Re is thought to be a more suitable material. Preliminary tests are underway to evaluate the ductility of different Mo-Re alloys. A Mo-11Re tube was successfully bent at room temperature, after which it was heated for four hours at 3000 °F. The tube then fractured when a subsequent attempt was made to bend it at room temperature. The tube was then bent at 392 °F. At this elevated temperature, the tube still fractured, but survived a bend of approximately 90° before fracture occurred. It is known that a higher rhenium content increases the ductility of molybdenum. Several alloys of molybdenum with higher percentages of rhenium content are now being considered for use as the heat-pipe container material.
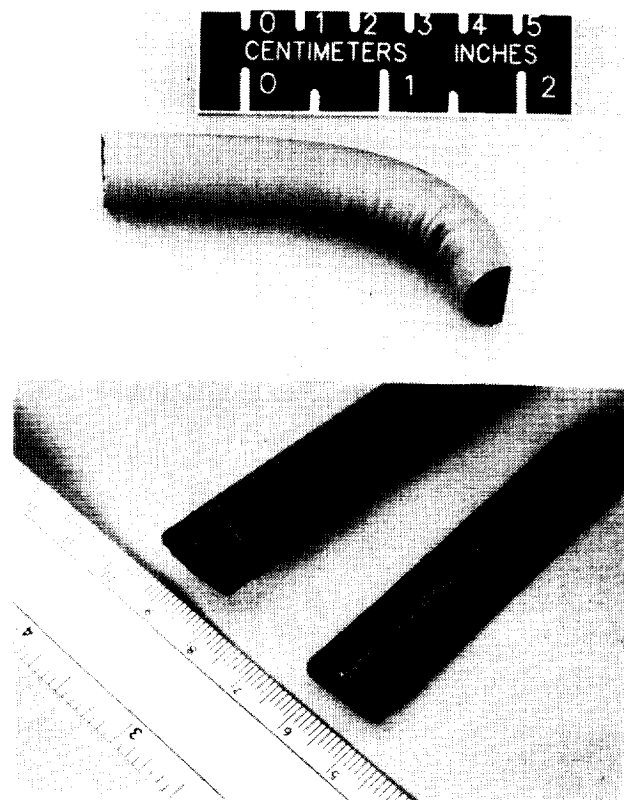

Figure 19. - Heat pipe fabrication.

EMBEDDING HEAT PIPES IN A REFRACTORY-COMPOSITE STRUCTURE

In the construction of the heat-pipe-cooled leading edge, several design considerations can be incorporated to reduce the thermal stresses and alleviate the potential problem of cracks in the C/SiC due to excessive through-the-thickness normal stresses. To reduce the heat pipe thermal stresses in the through-the-thickness and spanwise directions, a strain isolator can be placed between the heat pipe and the refractory-composite structure. If the strain isolator completely surrounds the heat pipe, it will add thermal resistance on the flat part of the heat pipe where heat is entering the heat pipe. In the stagnation region, this added thermal resistance cannot be tolerated because of the magnitude of heating there. However, if the strain isolator covers only the curved part of the heat pipe, as shown in figure 20, the heat pipe will be allowed to grow in the through-the-thickness, spanwise, and chordwise directions with minimal increase in maximum temperatures. For the uncooled designs, no heat is lost from the interior surface, so the thermal effect of the strain isolator should be negligible. In addition, the strain isolator will help reduce the stresses in the chordwise direction. As discussed previously, the heat pipe is expected to grow in the chordwise direction more than the refractory composite. A soft material can be placed at the ends of the heat pipes to allow for thermal expansion in the chordwise direction. The addition of a soft carbon strain isolator is similar in purpose to Thermo Electron's use of a soft carbon strain isolator sandwiched between W and SiC, in the construction of a ceramic liquid-metal heat pipe (refs. 19-20).

Tests are planned to evaluate the effectiveness of three different woven carbon preforms with strain isolators for reducing and surviving the thermal stresses. One preform that is being considered is a flat panel with webs that will be folded over the "D-shaped" heat pipe and strain isolator. The second preform being considered uses woven "D-shaped" channels through which the heat pipe and strain isolator will be inserted. The final preform being considered involves weaving the preform around a rectangular cross section consisting of the "D-shaped" heat pipe and a concave shaped strain isolator.
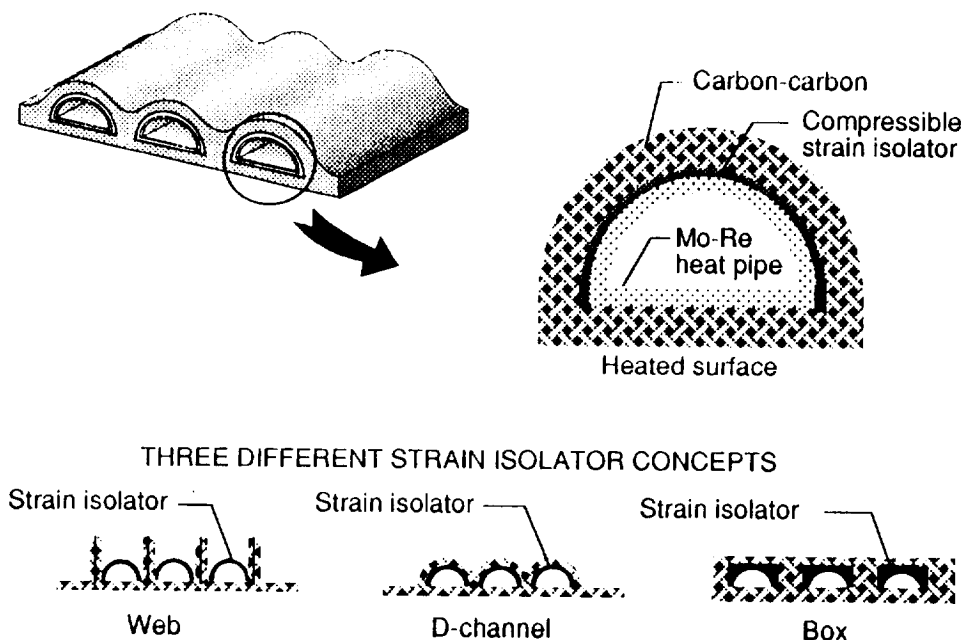

Figure 20. - Embedding heat pipes in a refractory-composite structure.

SUMMARY

Heat pipes have been considered for use on wing leading edge for over 20 years. Early concepts envisioned metal heat pipes cooling a metallic leading edge. Several superalloy/sodium heat pipes were fabricated and successfully tested for wing leading edge cooling. Results of radiant heat and aerothermal testing indicate the feasibility of using heat pipes to cool the stagnation region of shuttle-type space transportation systems. The test model withstood a total of seven radiant heating tests, eight aerothermal tests, and twenty-seven supplemental radiant heating tests. Cold-wall heating rates ranged from 21 to 57 Btu/ft^2-s and maximum operating temperatures ranged from 1090 to 1520 °F. Follow-on studies investigated the application of heat pipes to cool the stagnation regions of single-stage-to-orbit and advanced shuttle vehicles. Results of those studies indicate that a "D-shaped" structural design can reduce the mass of the heat-pipe concept by over 44 percent compared to a circular heat-pipe geometry. Simple analytical models for heat-pipe startup from the frozen state (working fluid initially frozen) were adequate to approximate transient, startup, and steady-state heat-pipe performance. Improvement in analysis methods has resulted in the development of a finite-element analysis technique to predict heat-pipe startup from the frozen state. However, current requirements of light-weight design and reliability suggest that metallic heat pipes embedded in a refractory composite material should be used. This concept is the concept presently being evaluated for NASP.

A refractory-composite/heat-pipe-cooled wing leading edge is currently being considered for the National Aero-Space Plane (NASP). This concept uses high-temperature refractory-metal/lithium heat pipes embedded within a refractory-composite structure and is significantly lighter than an actively cooled wing leading edge because it eliminates the need for active cooling during ascent and descent. Since the NASP vehicle uses cryogenic hydrogen to cool structural components and then burns this fuel in the combustor, hydrogen necessary for descent cooling only, when the vehicle is unpowered, is considered to be a weight penalty. Details of the design of the refractory-composite/heat-pipe-cooled wing leading edge are currently being investigated. Issues such as thermal contact resistance and thermal stress are also being investigated.

REFERENCES

1. Silverstein, C. C.: A Feasibility Study of Heat-Pipe-Cooled Leading Edges for Hypersonic Cruise Aircraft. NASA CR 1857, 1971.

2. Niblock, G. A.; Reeder, J. C.; and Huneidi, F.: Four Space Shuttle Wing Leading Edge Concepts. Journal of Spacecraft and Rockets, Vol. 11, No. 5, May 1974, pp. 314-320.

3. Alario, J. P. and Prager, R. C.: Space Shuttle Orbiter Heat Pipe Application. NASA CR-128498, 1972.

4. Anon.: Study of Structural Active Cooling and Heat Sink Systems for Space Shuttle. NASA CR-123912, 1972.

5. Anon.: Design, Fabrication, Testing, and Delivery of Shuttle Heat Pipe Leading Edge Test Modules. NASA CR-124425, 1973.

6. Camarda, Charles J.: Analysis and Radiant Heating Tests of a Heat-Pipe-Cooled Leading Edge. NASA TN D-8468, August 1977.

7. Camarda, Charles J.: Aerothermal Tests of a Heat-Pipe-Cooled Leading Edge at Mach 7. NASA TP-1320, November 1978.

8. Camarda, Charles J.; and Masek, Robert V.: Design, Analysis and Tests of a Shuttle-Type Heat-Pipe-Cooled Leading Edge. Journal of Spacecraft and Rockets, Vol. 18, No. 1, January-February, 1981.

9. Peeples, M. E.; Reeder, J. C.; and Sontag, K. E.: Thermostructural Applications of Heat Pipes. NASA CR-159096, 1979.

10. Boman, B. L.; Citrin, E. C.; Garner, E. C.; and Stone, J. E.: Heat Pipes for Wing Leading Edges of Hypersonic Vehicles. NASA CR-181922, January 1990.

11. Boman, B.; and Elias, T.: Tests on a Sodium/Hastelloy X Wing Leading Edge Heat Pipe for Hypersonic Vehicles. Presented at the AIAA/ASME 5th Joint Thermophysics and Heat Transfer Conference, June 18-20, 1990, Seattle, WA. AIAA-90-1759.

12. Colwell, Gene T.; Jang, Jong H.; and Camarda, Charles J.: Modeling of Startup from the Frozen State. Paper presented at the Sixth International Heat Pipe Conference, Grenoble, France, May 25-29,1987.

13. Glass, David E.; and Camarda, Charles J.: Results of Preliminary Design Studies of a Carbon-Carbon/Refractory-Metal Heat-Pipe Wing Leading Edge. NASP TM 1071, July 1989.

14. Glass, David E.; and Camarda, Charles J.: Preliminary Thermal/Structural Analysis of a Carbon-Carbon/Refractory-Metal Heat-Pipe-Cooled Wing Leading Edge. Paper Presented at the First Thermal Structures Conference, University of Virginia, Charlottesville, Virginia, November 13-15, 1990.

15. Dunn, P.; and Reay, D. A.: Heat Pipes. Pergamon Press, Oxford, 1982.

16. Chi, S. W.: Heat Pipe Theory and Practice. Hemisphere Publishing Corporation, Washington, D.C., 1976.

17. Cotter, T. P.: Heat Pipe Startup Dynamics. Heat Pipes, Volume XVI of AIAA Selected Reprint Series, edited by C. L. Tien, September 1973, pp. 42-45.

18. Whetstone, W. D.: EISI-EAL Engineering Analysis Language Reference Manual - EISI-EAL System Level 2091. Engineering Information Systems, Inc., July 1983.

19. Reagan, P.; Miskolczy, G.; and Huffman, F.: Development of a CVD Silicon-Carbide-Graphite-Tungsten Heat Pipe Structure. AIAA 16th Thermophysics Conference, Palo Alto, CA, June 23-25, 1981. AIAA-81-1160.

20. Reagan, Peter; Lieb, David; Miskolczy, Gabor; Goodale, Douglass; and Huffman, Fred: CVD Fabrication of Thermionic Converter and Heat Pipe, Ceramic Engineering and Science Proceedings, Vol. 4, July-August 1983, pp. 520-532.

21. Henson, M. C.; and Fetter, S. D.: Development of Refractory Materials for Actively Cooled Hypersonic Airframe Panels. Presented at the Tenth National Aero-Space Plane Technology Symposium, April 23-26, 1991. Paper No. 180.

22. Henson, M. C.; Adams, R. D.; Ahmad, A.; Fetter, S. D.; Kennedy, S. E.; Saathoff, W. M.; and Serinken, D. H.: Development of Refractory Composite Actively Cooled Panels for the NASP Airframe. Presented at the Ninth National Aero-Space Plane Technology Symposium, November 1-2, 1990. Paper No. 177.